Molecular Pharmacology Fast Forward. Published on January 19, 2006 as doi:10.1124/mol.105.020537
This article has not been copyedited and formatted. The final version may differ from this version.

Title:

Pseudolarix acid B, a novel tubulin-binding agent, inhibits angiogenesis by interacting with a distinct binding site on tubulin

Yun-Guang Tong, Xiong-Wen Zhang, Mei-Yu Geng, Jian-Ming Yue, Xian-Liang Xin, Fang Tian[1], Xu Shen, Lin-Jiang Tong, Mei-Hong Li, Chao Zhang, Wei-Hong Li, Li-Ping Lin, and Jian Ding

State Key Laboratory of Drug Research, Shanghai Institute of Materia Medica, Shanghai Institutes for Biological Science, Chinese Academy of Sciences, Shanghai 201203, P.R.China (Y-G T, X-W Z, J-M Y, F T, X S, L-J T, M-H L, C Z, W-H L, L-P L, J D); and Department of Pharmacology, Marine Drug and Food Institute, Ocean University of China, 5 Yushan Road, Qingdao 266003, China (M-Y G, X-L X)

Molecular Pharmacology Fast Forward. Published on January 19, 2006 as DOI: 10.1124/mol.105.020537
This article has not been copyedited and formatted. The final version may differ from this version.

Running Title: PAB inhibits angiogenesis by binding to a novel site on tubulin

Abbreviations: PAB, Pseudolarix acid B; HMEC, human microvascular endothelial cell; CAM, chorioallantoic membrane;

Address correspondence to: Dr. Jian Ding, Division of Anti-tumor Pharmacology, State Key Laboratory of Drug Research, Shanghai Institute of *Materia Medica*, Shanghai Institutes for Biological Sciences, Chinese Academy of Sciences, Shanghai 201203, Peoples Republic of China. E-mail: jding@mail.shcnc.ac.cn

Text pages: 26

Table: 1

Figures: 5

References: 43

Abstract: 181 words

Introduction: 431 words

Discussion: 883 words

Abstract

Tubulin-binding agents have received considerable interest as potential tumor-selective angiogenesis-targeting drugs. Herein, we report that pseudolarix acid B (PAB), isolated from the traditional Chinese medicinal plant *Pseudolarix kaempferi* Gordon, is a tubulin-binding agent. We further demonstrate that PAB significantly and dose-dependently inhibits proliferation, migration, and tube formation by human microvessel enthothelial cells. Notably, PAB eliminated newly formed endothelial tubes and microvessels both *in vitro* and *in vivo*. In addition, PAB dramatically arrested the cell cycle at G2/M phase. PAB also induced endothelial cell retraction, intercellular gap formation, and promoted actin stress fiber formation in conjunction with disruption of the tubulin and actin cytoskeletons. All of these effects occurred at noncytotoxic concentrations of PAB. We found that these effects of PAB are attributable to depolymerization of tubulin by direct interaction with a distinct binding site on tubulin as comparable with those of colchicine and vinblastine. Collectively, these findings show that PAB is a candidate antiangiogenic agent for use in cancer therapy, and they provide proof of principle for targeting this novel binding site on tubulin as a new strategy for treating cancer.

Introduction

Almost all aspects of angiogenesis require participation of the cytoskeleton, and accumulating evidence indicates that the cytoskeleton plays important roles in modulation of the physiological functions of blood vessels. The cytoskeleton, especially the microtubule and microfilament networks, is highly dynamic and is widely implicated in control of cell proliferation, migration, spreading, and elongation of endothelial cells (Ingber et al., 1995;Gottlieb et al., 1991). Therefore, changes in cytoskeletal dynamics, in particular the microtubules, are increasingly recognized as causing endothelial cells to undergo angiogenesis.

More than 300 agents have been reported to exhibit antiangiogenic activity, and clinical trials are currently being carried out on about 40 of these, including monoclonal antibodies(Hicklin et al., 2001), synthetic small molecules (Diane H.Boschelli, 1999), and natural products. Almost all of these antiangiogenic agents preferentially target growth factor-induced cell proliferation, apoptosis, migration, and thus angiogenesis. Little is known about compounds that target cytoskeletal changes involved in angiogenesis. In theory, compounds that affect cytoskeletal dynamics are promising antiangiogenic agents because they modulate critical endothelial cell functions, including motility, invasion, attachment, alignment, and proliferation. In fact, a variety of angiogenesis inhibitors currently under development, including endostatin, TNP-470, fumagillin, and thrombospondin-1, have been found to indirectly inhibit the endothelial cell cytoskeleton (Keezer et al., 2003). Therefore, targeting of cytoskeletal dynamics might lead to the development of new angiogenesis inhibitors (Salgaller, 2003).

Pseudolarix kaempferi is an indigenous plant of eastern China. The root bark of *P. kaempferi*, known as Tu-jin-Pi, is used as a traditional Chinese medicine for the treatment of microbial skin diseases. Pseudolarix acid B (PAB) is one of the most important natural diterpenoid compounds isolated from the root bark of *P. kaempferi* Gordon and is early known in China as an agent that causes the early termination of pregnancy. Our previous studies have demonstrated that PAB exhibits anti-angiogenesis via reducing HIF-1α using human umbilical vein endothelial cells

(Li Meihong et al). In principle, PAB might also be capable of inhibiting angiogenesis in other endothelial cell lines, and possibly via other mechanisms not as yet explored. In fact, we recently found that PAB triggers a dramatic arrest of the cell cycle at G2/M in HMEC cells. Given G2/M phase is strictly involved in dynamics of cytoskeleton, our findings might shed a new light on a mechanistic basis of PAB's angiogenesis-targeting activities. We therefore further selected HEMC cell line to unravel this hypothesis. We show that PAB inhibits angiogenesis both *in vitro* and *in vivo* by destabilizing the endothelial cytoskeleton, which was shown to be due to its binding to a distinct site on tubulin from those of colchicine and vinca alkaloids.

MATERIALS AND METHODS

Herbs and compound

PAB was isolated from the ethanolic extract of the root bark of *Pseudolarix kaempferi* by column chromatography and recrystallization, with the purity of 99.3% as determined by high-performance liquid chromatography. PAB was dissolved at a concentration of 0.01 mol/L in 100% DMSO as a stock solution, stored at -20°C. The structure of PAB is shown in Fig. 1.

Cells and cell culture

All reagents and media for cell culture were obtained from Sigma (St. Louis, MO, USA). HMECs were purchased from the American Type Culture Collection (Rockville, MD, USA) and cultured in MCDB131 containing 10% fetal bovine serum (FBS), 0.1 ng/ml EGF, and 1 μg/ml hydrocortisone.

HMEC proliferation assay

The effect of PAB on the growth of HMECs was measured using the sulforhodamine B (Sigma) method. Briefly, cells were plated in 96-well plates (5×10^3 cells/90 μl/well) in MCDB131 containing 20% FBS and cultured at 37°C for 24 h. Ten μl of serial dilutions of PAB was added and incubated for another 72 h. Cells were fixed by gentle addition of 100 μl cold (4°C) 10% trichloroacetic acid, and kept at 4°C for 1 h. The number of cells was estimated by the Sulforhodamine B assay. The inhibition of proliferation was calculated as $[1 - (A_{515\ treated}/A_{515\ control})] \times 100\%$.

HMEC migration assay

Migration of HMECs was determined in a transwell Boyden chamber (Costar, MA, Bedford, USA) containing a polycarbonate filter with a pore size of 8 μm(Ashton et al., 1999) coated with 0.2% gelatin. In the standard assay, a 0.1-ml cell suspension (2×10^5 cells/ml) containing PAB or 0.1% DMSO (v/v) was added to the upper compartment of each well. The lower compartment contained 0.6 ml MCDB131 supplemented with the same concentration of PAB or DMSO. After incubation for 8 h at 37°C, the filter was removed and fixed with ethanol. Cells on the lower surface of the filter (migrated) were stained with eosin and counted manually in five random fields. The inhibition of migration was calculated as $[1 - (\text{migrated cells}_{treated}/\text{migrated cells}_{control})] \times 100\%$.

Molecular Pharmacology Fast Forward. Published on January 19, 2006 as DOI: 10.1124/mol.105.020537
This article has not been copyedited and formatted. The final version may differ from this version.

HMEC tube formation assay

A tube formation assay was performed as usual. Briefly, a 96-well plate coated with 0.1 ml Matrigel (Becton Dickinson Labware, Bedford, MA) per well was allowed to solidify for 1 h at 37°C. Each well was seeded with 1×10^4 HMEC and cultured in MCDB131 containing various concentrations of PAB or 0.1% DMSO (v/v) for 24 h. Photographs from five randomly chosen fields were taken using an IX70 microscope (Olympus, Tokyo, Japan). The total length of the tube structures in each photograph was measured using Adobe Photoshop software (Soeda et al., 2000). Inhibition of tube formation was calculated as $[1 - (\text{tube length}_{\text{treated}} / \text{tube length}_{\text{control}})] \times 100\%$.

Rat aorta cultures

The thoracic aorta of Sprague–Dawley rats were dissected into 1-mm long rings, embedded in Matrigel, and incubated in serum-free endothelial cell basal medium containing 10 μg/ml gentamycin, 100 units/ml penicillin, 100 μg/ml streptomycin, and 0.25 μg/ml amphotericin (Nicosia and Ottinetti, 1990;Carlini et al., 1995). PAB were added on day 2, and the aorta rings were cultured for another 4 days. The medium was replaced every 24 h. Microvessel growth was photographed on day 6. To confirm the presence of endothelial cells in the microvessels, the rat aorta sections were immunohistochemically stained with 1:200 rabbit polyclonal antibody against the endothelial cell-specific marker CD31 (Santa Cruz Biotechnology, Santa Cruz, CA, USA).

Chicken chorioallantoic membrane (CAM) assay

Groups of 10 fertilized chicken eggs were transferred to an egg incubator (RX2TT, Lyon Inc., Chula Vista, CA, USA) maintained at 37°C and 50% humidity and grown for 9 days. The CAM was separated from the shell membrane by drilling two small holes, one at the broad end of the egg, where the air sac is located, and the second at a position 90 degrees from the first. Gentle suction was applied at the hole located on the broad end of the egg to create a false air sac directly over the CAM. A 1-cm^2 window was removed from the egg shell immediately over the second hole. Filter paper disks saturated with compounds or 0.1% DMSO (v/v) were placed on the areas between preexisting vessels, and the embryos were incubated for an additional

Molecular Pharmacology Fast Forward. Published on January 19, 2006 as DOI: 10.1124/mol.105.020537
This article has not been copyedited and formatted. The final version may differ from this version.

48 h. The neovascular zones under the disks were photographed at ×10 magnification under a stereomicroscope (Leica, MS5, New Jersey, USA). Angiogenesis was quantified by counting the number of blood vessel branch points on the photos.

Cell cycle assay

HMEC cells (1×10^6) were seeded into a 6-well plate and allowed to adhere overnight. PAB were added, and incubated for 24 h. One ml of cells suspended in PBS (1.5×10^6 cells) was mixed with 9 ml of 70% ethanol (stored at –20°C) in a tube on ice. Following centrifugation (1500 rpm), the cells were diluted with PBS and recentrifuged. The cell pellet was then suspended in a mixture of 0.5 ml PBS and 0.5 ml DNA extraction buffer (made by mixing 192 ml of 0.2 M Na_2HPO_4 with 8 ml of 0.1 M citric acid, pH 7.8). After incubation at room temperature for 5 min and centrifugation at 300 × g for 5 min, the cell pellet was suspended in 1 ml DNA-staining solution (50 μg/ml RNase, 0.5% Triton X-100, and 50 μg/ml propidium iodide) and incubated for 30 min at room temperature. Cell cycle distribution was determined using flow cytometry.

Microscopy

HMEC cells were seeded onto 12-mm circular glass coverslips precoated with 10 μg/ml collagen overnight, and then treated with PAB at different concentrations for different time. Cell membranes were permeabilized with 0.1% Triton X-100/PBS for 30 min and incubated with 1% bovine serum albumin for 30 min to reduce nonspecific staining. Filamentous actin was stained with 0.5 units/ml of Texas Red-X phalloidin (Molecular Probes Inc., Eugene, OR, USA) for 30 min. The tubulin cytoskeleton was labeled with a monoclonal anti-α-tubulin antibody (Molecular probes), followed by Alexa Fluor 488-conjugated goat anti-mouse antibody (Molecular Probes). Nuclei were stained with the fluorescent DNA binding agent DAPI. After three to five rinses in PBS, the slides were mounted with using Prolong antifade reagent (Molecular Probes).

The influence of PAB on actin polymerization/depolymerization dynamics in HMECs was evaluated by staining F- and G-actin using 10 μg/ml Alexa Fluor 488-conjugated phallotoxin and 5 units/ml Texas Red-conjugated DNase I,

respectively, which bind stoichiometrically to actin subunits (Knowles and McCulloch, 1992). The experimental protocol has been detailed previously (Nagy et al., 2001). The photographs were taken under identical conditions using a Leica TCS confocal microscope (Leica, Deerfield, IL). The red (F-actin) and green (G-actin) fluorescence intensities were quantified using Leica TCS SP2 2.5 1104 software (Leica, Deerfield, IL, USA).

***In vitro* tubulin polymerization assay**

Over 99% pure microtubule protein (12 μM, Cytoskeleton Inc., Denver, CO, USA) was mixed with different concentrations of PAB in PEM buffer (100 mM PIPES, 1 mM $MgCl_2$, and 1 mM EGTA) containing 1 mM GTP and 5% glycerol. Microtubule polymerization was monitored at 37°C by light scattering at 340 nm using a VERSAmax multi-well spectrophotometer. The plateau absorbance values were used for calculations.

Intrinsic tryptophan fluorescence of tubulin

Tubulin (2 μM) was incubated with 25 μM of PAB, or colchicines or vinblastine at 37°C for 30 min. The fluorescence measurements were performed using 295 nm as the excitation wavelength. We selected 295 nm as the excitation wavelength to specifically excite the tubulin tryptophan residues. When excited at 295 nm, tubulin displayed a typical emission spectrum with a maximum at 336 nm.

Circular dichroism (CD) spectroscopy

For CD spectral experiments, 2 μM tubulin in PEM buffer was mixed with 2.5 μM of PAB. After incubation at 37°C for 1 h, CD spectra were obtained at 25°C using a Jasco J-810 spectropolarimeter (J715，JASCO，Tokyo, Japan).

Conformational states of tubulin using bis-8-anilinonaphthalene-1-sulfonate (bis-ANS)

The interaction of PAB with tubulin (2 μM) was monitored by examining its effects on the intrinsic fluorescence of tubulin-bis-ANS complexes (Bhattacharyya and Wolff, 1975;Lee et al., 1975). Relative fluorescence intensities (excitation at 400 nm, emission at 450-600 nm) were obtained with a Hitachi F-2500

spectrofluorometer at 37°C using a constant-temperature circulating water bath. Blank values (buffer alone) were subtracted from all measurements. PAB (10 μM) alone had very low absorbance (0.011) at 400 nm.

Probe conformational states of tubulin by DNTB

The kinetics of sulfhydryl group modification were monitored colorimetrically at 412 nm (Ellmann, 1959). Tubulin (5 μM) was incubated with 10 μM PAB at 37ºC for 30 min, after which 300 mM DTNB was added. After a 1-h incubation, the number of modified sulfhydryl groups was determined using a molar extinction coefficient of 12,000.

Competitive Inhibition Assay

Colchicine binding to tubulin

Tubulin-colchicine complex was formed by incubating 3 μM tubulin with 3 μM colchicine for 30 min at 37ºC (excitation at 365 nm, emission at 435 nm) (Bhattacharyya and Wolff, 1974;Hastie, 1991). PAB (0-25 μM) was added to the preformed tubulin-colchicine complex, and fluorescence was determined after 60 min at 37ºC using a Hitachi F-2500 spectrofluorometer. Spectra were taken by multiple scans, and blank values (buffer alone) were subtracted from all measurements.

Vinblastine binding to tubulin

Vinblastine (3 μM) containing a trace of [^{3}H] vinblastine (specific activity = 11 Ci/mmol) was mixed with tubulin (3 μM) and PAB (0-25 μM). The mixtures were incubated at 37ºC for 40 min, and bound vinblastine was determined using a DE-81 filter paper assay following Wilson's method (Wilson et al., 1975).

Molecular Pharmacology Fast Forward. Published on January 19, 2006 as DOI: 10.1124/mol.105.020537
This article has not been copyedited and formatted. The final version may differ from this version.

RESULTS

PAB inhibits three main steps of angiogenesis of HEMCs *in vitro*

We first investigated the effects of PAB on the three main steps of angiogenesis *in vitro*. Results indicated that PAB at indicated concentrations significantly and dose-dependently abrogated the proliferation, migration and tube formation of HMECs.

PAB inhibits the proliferation of HMECs

We initially investigated the effect of PAB on endothelial cell proliferation. HMECs were treated with 0.313, 0.625, 1.25, 2.5, and 5 μM PAB for 24 or 72 h. Except for the 24-h treatments with 0.313 and 0.625 μM, all concentrations of PAB caused a significant and dose-dependent suppression of HMEC proliferation (Fig. 2a). In addition, treatment with 5 μM PAB for 12, 24, 48, and 72 h resulted in a dramatic, time-dependent inhibition of cell proliferation, with inhibition of 7.5%, 47.8%, 60.8%, and 79.0%, respectively (Fig. 2b).

PAB inhibits the migration of HMECs

The migration of endothelial cells is a process of chemotaxis, which is indispensable in angiogenesis. We used a Boyden chamber assay to assess the ability of PAB to affect the migration of HMECs. We found that stimulation with 10% FBS for 8 h caused a large number of HMECs to migrate to the lower side of the filter in the Boyden chamber. Treatment with PAB (0.313, 0.625, 1.25, 2.5, and 5 μM) resulted in a dose-dependent suppression of cell migration (25.8%, 41.9%, 63.8%, 70.9%, and 80.8% inhibition, respectively; Fig. 2a and c).

PAB disrupts tube formation

We next evaluated the effect of PAB on the formation of functional tubes by HMECs plated on Matrigel. Matrigel provides endothelial cells a perfect environment for differentiation into an extensive and enclosed network of tubes. As shown in the Fig.2 c, the tube structure was severely destructed and displayed an incomplete and sparse tube network when incubate with PAB at 1.25 μM as compared with the control group. PAB (0.313, 0.625, 1.25, 2.5, and 5 μM) caused a dose-dependent inhibition of FBS-induced HMECs tube formation (41.32%, 59.3%,

82.6%, 87.7%, and 91.0% inhibition, respectively; Fig. 2a). This effect of PAB on tube formation was significantly more potent than on HMEC proliferation. Importantly, a noncytotoxic concentration (0.313 μM) of PAB inhibited migration by 25.8% and tube formation by 41.3%; therefore, the inhibitive effect of PAB on HMEC cell migration and tube formation was not due to cytotoxicity.

PAB is antiangiogenic both *ex vivo* and *in vivo*

PAB reduces sprout outgrowth and disrupts newly formed microvessels in rat aorta

Microvessels grow from rat aorta sections when they are embedded in Matrigel and cultured under appropriate conditions. This event is the result of a combination of endothelial cell proliferation, migration, and tube formation, which provides a close approximation of the process of angiogenesis *in vivo*. Staining for CD31 showed the development of microvessels occurred after 2 or 3 days incubation (data not shown). Treatment with PAB at 1.25 and 2.5 μM caused a significant retardation of this process. PAB at high concentrations (5 and 10 μM) triggered the regression of microvessels. In addition, treatment with PAB at 2.5 μM for 8 h caused the newly formed tubes to collapse, with complete collapse observed at 16 h (Fig. 2d).

PAB reduces neovascularization of the CAM

The CAM of the chicken embryo provides a unique model for investigating the process of new blood vessel formation and vessel responses to antiangiogenic agents. Using this model, we examined the *in vivo* antiangiogenic activity of PAB. A 48-h treatment of PAB caused a dose-dependent decrease in the branching of blood vessels. PAB at 5 nmol/egg showed a stronger effect than suramin at 125 nmol/egg (a potent angiogenesis inhibitor currently in phase II clinical trial) (Fig. 2e).

PAB arrests the cell cycle at G2/M phase

We next investigated whether PAB influences the endothelial cell cycle, which might provide insight into the mechanism of the antiangiogenic activity of PAB. PAB produces a concentration-dependent accumulation of cells in the G2/M phase of the cell cycle (Table 1). PAB (0.5 μM, 1 μM) caused 53.3% and 84.2% of the cells arrested in G2/M respectively, as compared with 22.8% of the controls.

PAB disrupts the cytoskeleton and alters the morphology of HMECs

We then reasoned that the induction of G2/M arrest by PAB is attributed to the disruption of the cytoskeleton. To test this hypothesis, we initially examined the effect of PAB on the organization of microtubules and F-actin, respectively, and then used merging images to illustrate the colocalization of these interested two molecules in response to PAB. As shown in Fig. 3a, PAB led to a dramatic disruption of the HMEC cytoskeleton, producing a diffuse microtubule network and an increase in actin stress fibers. Notably, both mitotic and interphase microtubules were lost following treatment with 10 μM PAB for 24 h, suggesting nearly complete depolymerization of the microtubule cytoskeleton by PAB. At the same concentrations that triggered changes in the cytoskeleton, PAB caused cell retraction, and formation of intercellular gaps (Fig. 3b).

Next, we examined the effects of PAB on F-actin. PAB caused a dose- and time-dependent enhancement of actin stress fiber formation across the cell body (Fig 3a). In addition, we found that a 30-min treatment with 1 μM PAB significantly (2.1-fold) increased the F-/G-actin ratio. The F-/G-actin ratio reached a maximum of a 3.1-fold increase after 8 h (Fig. 3c).

PAB inhibits tubulin polymerization *in vitro*

PAB has been shown to inhibit HMEC proliferation by depleting the cellular microtubule network. Thus, we were interested in arguing the effects of PAB on tubulin and actin polymerization *in vitro*. We first analyzed the influence of PAB on the polymerization of tubulin into microtubules *in vitro*. Purified tubulin alone (12 μM) was polymerized, while PAB inhibited the rate and extent of tubulin polymerization in a concentration-dependent manner (Fig. 4a). For example, 10 μM PAB decreased the steady-state polymer level by 45%. The percent inhibition of microtubule polymerization was calculated using the steady-state absorbance readings in the absence and presence of different concentrations of PAB (Fig. 4b).

PAB induces unique conformational changes in tubulin by binding to a novel site

PAB enhances the intrinsic tryptophan fluorescence of tubulin

The finding that PAB inhibits microtubule polymerization *in vitro* suggested that it binds to tubulin. To validate this hypothesis, we initially investigated the effects of PAB on the intrinsic tryptophan fluorescence of tubulin. Tubulin has eight tryptophan residues distributed throughout the primary structure. The intrinsic tryptophan fluorescence of tubulin reflects the dynamics of this protein. As shown in Fig. 5a, PAB (25 μM) enhanced the intrinsic tryptophan fluorescence of tubulin. In contrast, vinblastine and colchicines at same concentrations (25 μM) reduced the intrinsic tryptophan fluorescence of tubulin.

CD spectra show that PAB causes a unique conformational change in tubulin

The direct interaction of PAB with tubulin was further investigated using Far-UV CD spectroscopy which is generally used to measure the secondary structure of the protein. As shown in Fig. 5b, PAB triggered a change in the far-UV CD spectrum of tubulin, characterized by the alteration of helical content in tubulin. This finding suggests that PAB binds to tubulin, leading to a unique conformational change.

PAB enhances tubulin-bis-ANS fluorescence

The hydrophobic molecule bis-ANS binds stoichiometrically to tubulin and inhibits microtubule assembly (Horowitz et al., 1984). The extreme environmental sensitivity of bis-ANS makes it a useful probe for examining the conformational states of the tubulin dimer. PAB (25 μM) increased the tubulin-bis-ANS fluorescence by 60%. Furthermore, incubation of tubulin with bis-ANS prior to the addition of PAB produced similar results (data not shown). But, under identical conditions, vinblastine and colchicine had no effect on the fluorescence intensity (Fig. 5c).

PAB does not effect the chemical modification of tubulin cysteines by DNTB

The tubulin sulfhydryls are composed of a reactive function on a protein; specifically a thiol group on a cysteine residue. Because these sulfhydryl groups appear to be located in regions of tubulin that are important for polymerization, the changes in the chemical reactivity of these residues can be used as a measure of

conformational change. Binding of colchicine and its analogs causes a dramatic decrease in the reactivity of the cysteine residues (Roychowdhury et al., 2000). Similarly, vinblastine and its analogs suppress the reaction of tubulin with DTNB (Schmitt and Kram, 1978). We found that the accessibility of the DTNB-titratable cysteines was increased in the presence of PAB, although the total number of titratable cysteines was not apparently affected by PAB (Fig. 5d). Therefore, we conclude that the inhibition of microtubule polymerization by PAB is not due to modification of sulfhydryl groups, instead, binding to a novel site on tubulin.

PAB binds to a distinct binding site on tubulin from well-recognized ones

A large number of chemically diverse structures bind to tubulin *in vitro* and inhibit microtubule polymerization in cells and *in vitro*. The binding sites for the vinca alkaloid and colchicines appear to be important because most of the tubulin-binding compounds discovered bind to one of them (Correia and Lobert, 2001; Jordan et al., 1998). Thus, we preferentially examined whether PAB can share with the colchicines' or vinblastine' site of soluble tubulin.

Because colchicine is weakly fluorescent in aqueous solution, but it becomes strongly fluorescent when it binds to tubulin (Bhattacharyya and Wolff, 1974; Hastie, 1991), we used the fluorescence of tubulin-colchicine complexes to determine whether PAB shares a binding site with colchicine. PAB did not cause a significant change in the fluorescence triggered by colchicine, suggesting that it does not share a binding site with colchicine. The positive control, podophyllotoxin (25 μM), however, reduced the fluorescence by 35% (Fig. 5e). In addition, we found that colchicines could also bind to the tubulin-PAB complex (Fig. 5f), further supporting that the two compounds do not compete for the same binding site.

We next investigated whether PAB competitively inhibits the binding of [^{3}H] vinblastine to tubulin. We found that PAB did not inhibit vinblastine binding at the concentrations examined (1-25 μM; Fig. 5g). In contrast, 1-10 μM vincristine, an analog of vinblastine, significantly inhibited vinblastine binding to tubulin (60% inhibition at 10 μM vincristine). These results demonstrate that PAB does not bind to the vinblastine-binding site.

Molecular Pharmacology Fast Forward. Published on January 19, 2006 as DOI: 10.1124/mol.105.020537
This article has not been copyedited and formatted. The final version may differ from this version.

DISCUSSION

Angiogenesis is the formation of new blood vessels from the endothelium of the existing vasculature. Tumor growth and metastasis are angiogenesis-dependent; hence, blocking angiogenesis has been considered as a strategy for arresting tumor growth （Matter A., 2001）. This possibility has stimulated intensive research and the development of antiangiogenic molecules. Here, we showed that PAB can inhibit all three steps of angiogenesis (endothelial cell proliferation, migration, and tube formation) at noncytotoxic doses. In addition, PAB nearly eliminated all sprout growth and showed potent antiangiogenic effects in the *in vivo* CAM model. The unique antiangiogenic effect of PAB is highlighted by its ability to eliminate newly formed endothelial tubes and microvessels and to arrest the cell cycle in G2/M phase. Since G2/M phase is strictly involved in dynamics of cytoskeleton, our findings might shed a new light on a mechanistic basis of PAB's angiogenesis-targeting activities.

The cytoskeleton has long been of interest in cancer chemotherapy because it is targeted by several well-validated antimitotic agents (Peterson and Mitchison, 2002). Because morphological changes in endothelial cells, such as spreading and elongation, are crucial for endothelial cell tube formation, and particularly the special role of the cytoskeleton in endothelial cell function has recently become clearer, the endothelial cytoskeleton has received attention as a therapeutic target for antiangiogenic strategies (Ingber et al., 1995;Gottlieb et al., 1991).

The cytoskeleton mainly consists of microfilaments and microtubules, which form a dynamic framework that maintains cell shape (Ingber et al., 1995). Therefore, preferentially targeting the HMEC cytoskeletal system might account for the antiangiogenic potential of certain agents. In our studies, PAB disrupted the organization of both microfilaments and microtubules in HMECs. In the presence of PAB, the microtubule network in HMECs was diffuse and was accompanied by a decrease in G-actin due to an increase in the formation of actin stress fibers. These findings were paralleled by changes in morphology, including endothelial cell retraction, intercellular gap formation, and membrane blebbing. Because microtubules

are strictly involved in the maintenance of cell shape, and the disruption of the microtubular network leads to rapid rounding up of cells, the morphological and cytoskeletal changes induced by PAB appear to be due to the dynamic alterations in the microtubule network. Indeed, we found that, even at nontoxic concentrations, PAB inhibited the tubulin polymerization *in vitro*. We suspect that this mechanism underlies the ability of PAB to cause cell retraction, membrane blebbing, and subsequent disruption of the cytoskeleton.

Microfilaments are contractile structures and consist of actin either in monomeric (G-actin) or filamentous form (F-actin) (Gottlieb et al., 1991;Kunze and Rustow, 1993). The monomeric status of the actin cytoskeleton favors endothelial cell migration. PAB facilitated the formation of actin stress fibers, preventing the shift of actin to a monomeric state. This accounts for its ability to suppress endothelial cell migration. Several studies have demonstrated that cooperation between microtubules and the actin cytoskeleton is crucial in the control of cell shape, contraction, and motility. However, a better understanding of the contribution of PAB to the intrinsic relationship between actin and microtubule cytoskeleton needs further elucidation.

The ability of compounds to block cells in G2/M phase is consistent with a disruption of cytoskeleton via binding to tubulin (Schneider et al., 2003). PAB enhanced the intrinsic tryptophan fluorescence of tubulin. This perturbed tubulin conformation occurred in the vicinity of tryptophan residues was likely due to its direct binding to tubulin. The altered helical content in tubulin triggered by PAB using Far-UV CD spectrum provide additional evidence supporting this conclusion. A large number of substances with chemically diverse structures have been identified to bind to tubulin and inhibit microtubule polymerization *in vitro* and in cells. The *Vinca* alkaloid site and the colchicine site are two important drug binding sites in soluble tubulin, and many of the microtubule depolymerizing agents bind to one of these sites (Jordan et al., 1998). Interestingly, we found that neither vinblastine nor colchicines competitively inhibited the binding of PAB to tubulin, suggesting that PAB may bind to a distinct binding site on tubulin from these well-recognized ones. In fact, the differently functional profiles of PAB on both tubulin-bis-ANS fluorescence and

DTNB's chemical modification of titratable cysteines of tubulin further support this notion. Recently, Wong et. al reported that PAB could arrest tumor growth via targeting tubulin (Wong et al., 2005). However, their observations that PAB could replace colchicines only at high concentrations made them hesitate to come to a definite conclusion on this issue, since non-specific binding cannot exclude out under this condition.

In summary, we have shown for the first time that PAB binds to a distinct binding site(s) on tubulin. This underlies its antiangiogenic activities, which include alteration in endothelial cell morphology, destabilization of the tubulin cytoskeleton, and disruption of newly formed tubules and microvessels both *in vitro* and *in vivo*. These findings, together with its low toxicity *in vivo* (LD_{50} of 486 mg/kg in mice) (unpublishing data), indicate that PAB is a promising tubulin-binding, antiangiogenic compound. In addition, the impact of PAB disrupting the newly formed microvessels might also underscore its potential involvement in vascular-targeting activity. Further identification of the binding consensus sequences of the PAB binding site on tubulin is needed, with the aim of the structure-assisted development of new tubulin-binding agents, especially compounds that have potential targeting both angiogenic and vascular activities.

Acknowledgements

We thank Ms. Wei Bian, Institute of Biochemistry and Cell Biology (Shanghai, P.R.China), for her skillful assistance with the Leica TCS confocal microscope.

References

Ashton, A.W., R.Yokota, G.John, S.Zhao, S.O.Suadicani, D.C.Spray, and J.A.Ware. (1999). Inhibition of endothelial cell migration, intercellular communication, and vascular tube formation by thromboxane A(2). *J. Biol. Chem.* 274:35562-35570.

Bhattacharyya, B. and J.Wolff.(1974). Promotion of fluorescence upon binding of colchicine to tubulin. *Proc. Natl. Acad. Sci. U. S. A* 71:2627-2631.

Bhattacharyya, B. and J.Wolff. (1975). The interaction of 1-anilino-8-naphthalene sulfonate with tubulin: a site independent of the colchicine-binding site. *Arch. Biochem. Biophys.* 167:264-269.

Carlini, R.G., A.A.Reyes, and M.Rothstein. (1995). Recombinant human erythropoietin stimulates angiogenesis in vitro. *Kidney Int.* 47:740-745.

Correia, J.J. and S.Lobert. (2001). Physiochemical aspects of tubulin-interacting antimitotic drugs. *Curr. Pharm. Des* 7:1213-1228.

Davy, D. A., H. D. Campbell, S. Fountain, D.de Jong, and M. F.Crouch. (2001). The flightless I protein colocalizes with actin- and microtubule-based structures in motile Swiss 3T3 fibroblasts: evidence for the involvement of PI 3-kinase and Ras-related small GTPases. J.Cell Sci., 114: 549-562,.

Diane H.Boschelli. (1999). Small molecule inhibitors of receptor tyrosine kinases. *Drugs of the Future* 4:515-537.

Ellmann, G.L. (1959). Tissue sulfhydryl groups. *Arch. Biochem. Biophys.* 82:70-77.

Essler, M., K.Hermann, M.Amano, K.Kaibuchi, J.Heesemann, P.C.Weber, and M.Aepfelbacher. (1998). Pasteurella multocida toxin increases endothelial permeability via Rho kinase and myosin light chain phosphatase. *J Immunol.* 161:5640-5646.

Garcia, J.G., H.W.Davis, and C.E.Patterson. (1995). Regulation of endothelial cell gap formation and barrier dysfunction: role of myosin light chain phosphorylation. *J Cell Physiol* 163:510-522.

Goode, B. L., D. G Drubin, and G. Barnes. (2000). Functional cooperation between the microtubule and actin cytoskeletons. Curr.Opin.Cell Biol., *12:* 63-71,

Gottlieb, A.I., B.L.Langille, M.K.Wong, and D.W.Kim. (1991). Structure and function of the endothelial cytoskeleton. *Lab Invest* 65:123-137.

Hastie, S.B. 1991. Interactions of colchicine with tubulin. *Pharmacol Ther* 51:377-401.

Hicklin, D.J., L.Witte, Z.Zhu, F.Liao, Y.Wu, Y.Li, and P.Bohlen. (2001). Monoclonal antibody strategies to block angiogenesis. *Drug Discov. Today* 6:517-528.

Holzinger, A. (2001). Jasplakinolide. An actin-specific reagent that promotes actin polymerization. *Methods Mol. Biol.* 161:109-120.

Horowitz, P., V.Prasad, and R.F.Luduena. (1984). Bis(1,8-anilinonaphthalenesulfonate). A novel and potent inhibitor of microtubule assembly. *J. Biol. Chem.* 259:14647-14650.

Ingber, D.E., D.Prusty, Z.Sun, H.Betensky, and N.Wang. (1995). Cell shape, cytoskeletal mechanics, and cell cycle control in angiogenesis. *J. Biomech.* 28:1471-1484.

Jordan, A., J.A.Hadfield, N.J.Lawrence, and A.T.McGown. (1998). Tubulin as a target for anticancer drugs: agents which interact with the mitotic spindle. *Med. Res. Rev.* 18:259-296.

Keezer, S.M., S.E.Ivie, H.C.Krutzsch, A.Tandle, S.K.Libutti, and D.D.Roberts. (2003). Angiogenesis inhibitors target the endothelial cell cytoskeleton through altered regulation of heat shock protein 27 and cofilin. *Cancer Res.* 63:6405-6412.

Knowles, G.C. and C.A.McCulloch. (1992). Simultaneous localization and quantification of relative G and F actin content: optimization of fluorescence labeling methods. *J. Histochem. Cytochem.* 40:1605-1612.

Kunze, D. and B.Rustow. (1993). Pathobiochemical aspects of cytoskeleton components. *Eur. J. Clin Chem. Clin Biochem.* 31:477-489.

Kuriyama, R. and H.Sakai. (1974). Role of tubulin-SH groups in polymerization to microtubules. Functional- SH groups in tubulin for polymerization. *J. Biochem.* 76:651-654.

Lee, J.C., D.Harrison, and S.N.Timasheff. (1975). Interaction of Vinblastine with Calf Brain Microtubule protein. *J. Biol. Chem.* 250:9276-9282.

Luduena, R.F. and M.C.Roach. (1991). Tubulin sulfhydryl groups as probes and targets for antimitotic and antimicrotubule agents. *Pharmacol. Ther.* 49:133-152.

Matter A. (2001). Tumor angiogenesis as a therapeutic target. *Drug Discorvery Today.* 6: 1005-1024.

Nagy, N., C.Brenner, N.Markadieu, C.Chaboteaux, I.Camby, B.W.Schafer, R.Pochet, C.W.Heizmann, I.Salmon, R.Kiss, and C.Decaestecker. (2001). S100A2, a putative tumor suppressor gene, regulates in vitro squamous cell carcinoma migration. *Lab Invest* 81:599-612.

Nicosia, R.F. and A.Ottinetti. (1990). Growth of microvessels in serum-free matrix culture of rat aorta. A quantitative assay of angiogenesis in vitro. *Lab Invest* 63:115-122.

Peterson, J.R. and T.J.Mitchison. (2002). Small molecules, big impact. A history of chemical inhibitors and the cytoskeleton. *Chem. Biol.* 9:1275-1285.

Prasad, A.R., R.F.Luduena, and P.M.Horowitz. (1986). Bis(8-anilinonaphthalene-1-sulfonate) as a probe for tubulin decay. *Biochemistry* 25:739-742.

Roychowdhury, M., N.Sarkar, T.Manna, S.Bhattacharyya, T.Sarkar, P.Basusarkar, S.Roy, and

B.Bhattacharyya. (2000). Sulfhydryls of tubulin. A probe to detect conformational changes of tubulin. *Eur. J. Biochem.* 267:3469-3476.

Salgaller, M.L. (2003). Technology evaluation: bevacizumab, Genentech/Roche. *Curr. Opin. Mol. Ther.* 5:657-667.

Schmitt, H. and R.Kram. (1978). Binding of antimitotic drugs around cysteine residues of tubulin. *Exp. Cell Res*. 115:408-411.

Schneider, Y., P.Chabert, J.Stutzmann, D.Coelho, A.Fougerousse, F.Gosse, J.F.Launay, R.Brouillard, and F.Raul. (2003). Resveratrol analog (Z)-3,5,4'-trimethoxystilbene is a potent anti-mitotic drug inhibiting tubulin polymerization. *Int. J. Cancer* 107:189-196.

Soeda, S., T.Kozako, K.Iwata, and H.Shimeno. (2000). Oversulfated fucoidan inhibits the basic fibroblast growth factor- induced tube formation by human umbilical vein endothelial cells: its possible mechanism of action. *Biochim. Biophys. Acta* 1497:127-134.

Theriot, J.A. and T.J.Mitchison. (1991). Actin microfilament dynamics in locomoting cells. *Nature* 352:126-131.

Tong, Y., X.Zhang, F.Tian, Y.Yi, Q.Xu, L.Li, L.Tong, L.Lin, and J.Ding. (2005). Philinopside A, a novel marine-derived compound possessing dual anti-angiogenic and anti-tumor effects. *Int. J. Cancer* 114:843-853.

Tong, Y., X.Zhang, W.Zhao, Y.Zhang, J.Lang, Y.Shi, W.Tan, M.Li, Y.Zhang, L.Tong, H.Lu, L.Lin, and J.Ding. (2004). Anti-angiogenic effects of Shiraiachrome A, a compound isolated from a Chinese folk medicine used to treat rheumatoid arthritis. *Eur. J. Pharmacol*. 494:101-109.

Ward, L.D. and S.N.Timasheff. (1994). Cooperative multiple binding of bisANS and daunomycin to tubulin. *Biochemistry* 33:11891-11899.

Wang, W.C., R.F. Lu, S.X. Zhao, Y.Z. Zhu. (1982). Antifertility effect of pseudolarix acid B. *Acta Pharm. Sin*. 3: 188– 192.

Wang, W.C., R.F. Lu, S.X. Zhao, and Z.P. Gu. (1988). Comparison of early regnancy-terminating effect and toxicity between pseudolarix acids A and B. *Acta Pharm. Sin*. 9: 445–448.

Wang, W.C., Z.P. Gu, A. Koo, and W.S. Chen. (1991). Effects of pseudolaric acid B on blood flows of endometrium and myometrium in pregnant rats. *Acta Pharm. Sin.* 12:423– 425.

Wilson, L., K.M.Creswell, and D.Chin. (1975). The mechanism of action of vinblastine. Binding of [acetyl- 3H]vinblastine to embryonic chick brain tubulin and tubulin from sea urchin sperm tail outer doublet microtubules. *Biochemistry* 14:5586-5592.

Wong, V.K.W. Pauline Chiu, Stephen S.M. Chung, LarryM.C. Chow,Yun-Zhe Zhao, Burton B.Yang,

and Ben C.B. Ko. (2005). Pseudolaric acid B, a novel microtubule-destabilizing agent that circumvents multidrug resistance phenotype and exhibits antitumor activity in vivo. *Clin. Cancer Res.* 11:6002-6011.

Footnotes:

This project was supported by grants of High Tech Research and Development Program (No. 2002AA2Z346A); the Knowledge Innovation Program of Chinese Academy of Sciences (No. KSCX2-SW-202, No. KSCX2-3-07-8) and the National Natural Science Foundation (No. 30228032 and No. 30228032).

Molecular Pharmacology Fast Forward. Published on January 19, 2006 as DOI: 10.1124/mol.105.020537
This article has not been copyedited and formatted. The final version may differ from this version.

Figures and Legends

Figure 1 Chemical structure of PAB

Figure 2 **PAB inhibits angiogenesis *in vitro, ex vivo* and *in vivo.*** (a) Effect of PAB on HMEC cell proliferation. Proliferation of HMEC cells were was examined after 24 (●) and 72 h (■). Also, migration (◆) and tube formation (▲) were assessed. Values represent the means ± SD of triplicate measurements. (b) Time-dependent inhibition of HMEC proliferation by 5 μM PAB. Values represent the means ± SD of triplicate measurements. (c) Effect of PAB on tube formation and migration by HMEC. HMECs were seeded in Matrigel-coated 96-well plates and incubated for 24 h with (A and C) medium alone or (B and D) 1.25 μM PAB. In A and B, microscopic images were obtained from five randomly chosen fields, and panels C and D show HMEC migration. (d) Effect of PAB on microvessel outgrowth arising from rat aorta sections. Fresh thoracic aorta from Sprague-Dawley rats was sliced into 1-mm thick sections. The sections were embedded in Matrigel and cultured in DMEM for 24 h. On day 2, cells received no addition (A) or 2.5 μM PAB (B), and microvessel growth was photographed on day 6. (e) Effect of PAB on CAM. Fertilized eggs were incubated continuously for 9 days, after which a window was opened to expose the CAM. PAB was added, and the eggs were incubated for another 48 h with 0.1% DMSO (A) or 10 nmol/egg (B). The treated CAM was then harvested and photographed. Angiogenesis was quantified by counting the number of blood vessel branch points in each photograph (C). Each value represents the mean ± SD of 10 eggs. *P<0.01 *vs.* control.

Figure 3 Effect of PAB on the HMEC cell cytoskeleton and cell morphology. (a) Effect of PAB alone on the cytoskeleton. HMECs were seeded onto 12-mm circular glass coverslips that were precoated with 10 μg/ml collagen. The cells were allowed to adhere overnight before treatment for 4 or 8 h with or without 1 μM PAB. Cells were fixed and stained for microtubules (green), F-actin (red) and nuclei (blue). (b)

Effects of PAB on cell morphology. Confluent HMECs cells were treated with 1 μM PAB for 4 h. The cell morphology were photographed using an IX70 microscope (Olympus, Tokyo, Japan). (c) Measurement of changes in the levels of F-/G-actin in response to 1 μM PAB at different time points. Levels of F- and G-actin were determined by staining with 10 μg/ml Alexa Fluor 488-conjugated phallotoxin and 5 units/ml Texas Red-conjugated DNase I, respectively.

Figure 4 Effects of PAB on microtubule and actin polymerization. (a) Polymerization of microtubules in various concentrations of PAB was recorded continuously for 30 min by measuring the absorbance at 340 nm. (b) Turbidity of microtubule protein incubated for 30 min at 37°C with various concentrations of PAB as determined by absorbance at 340 nm.

Figure 5 PAB induces unique conformational changes in tubulin by binding to a site different with colchicine and vinblastine. (a) Enhancement of intrinsic tryptophan of tubulin by PAB. Tubulin (2 μM) was incubated with 25 μM of PAB, colchicines or vinblastine at 37°C for 30 min. The fluorescence measurements were performed using 295 nm. (b) Far-UV CD spectra of tubulin in the presence of PAB. Tubulin (2 μM) in PEM buffer was mixed with 2.5 μM of PAB. After incubation at 37°C for 1 h, CD spectra were obtained using a Jasco J-810 spectropolarimeter. (c) Enhancement of tubulin-ANS complex fluorescence by PAB. Tubulin (2 μM) was mixed for 30 min at 37°C in the absence or presence of 25 μM PAB, colchicine or vinblastine. Bis-ANS (15 μM) was then added, and fluorescence was measured after 15 min of incubation (excitation at 400 nm, emission at 450-600 nm). (d) Effect of PAB on sulfhydryl reactivity of tubulin. Tubulin (5 μM) was incubated for 30 min at 37°C in the absence or presence of 10 μM PAB, colchicine or vinblastine, after which the solution was adjusted to 300 μM DTNB. The kinetics of sulfhydryl group modification was monitored for 40 min by measuring the absorbance at 412 nm. (e) Effects of PAB on the colchicine binding site. Tubulin (3 μM) was incubated with 3 μM colchicine for 30 min at 37°C to form tubulin-colchicine complexes. The solution was mixed for 60 min at 37°C with various concentrations of PAB (▲;

0-25 μM) or polophyllotoxin (■; 0-25 μM). Fluorescence spectra were recorded (excitation at 365 nm, emission at 390nm. (f) Effect of colchicine on PAB-tubulin complex. Tubulin (3 μM) was incubated with various concentration of PAB for 30 min at 37°C, then the solution was incubated for 60 min at 37°C with 3 μM colchicine. Fluorescence spectra were recorded as above. (g) Effects of PAB on the vinblastine binding site. Vinblastine (3 μM) containing a trace of [^{3}H] vinblastine was mixed for 30 min with 3 μM tubulin, after which the solution was incubated for 60 min with various concentrations of PAB (▲; 0-25 μM) or vincristine (■; 0-10 μM). Bound vinblastine was determined using a filter-binding assay.

Molecular Pharmacology Fast Forward. Published on January 19, 2006 as DOI: 10.1124/mol.105.020537
This article has not been copyedited and formatted. The final version may differ from this version.

Table 1 Effect of PAB on mitosis in HMEC cells.

PAB (μM)	Cell cycle distribution (%)		
	G1	S	G2/M
0	42.2±1.4	34.9±0.4	22.8±1.0
0.5	23.8±7.3	22.9±1.6	53.3±8.9
1	2.5±0.1	13.8±0.7	84.2±0.2

Figure 1

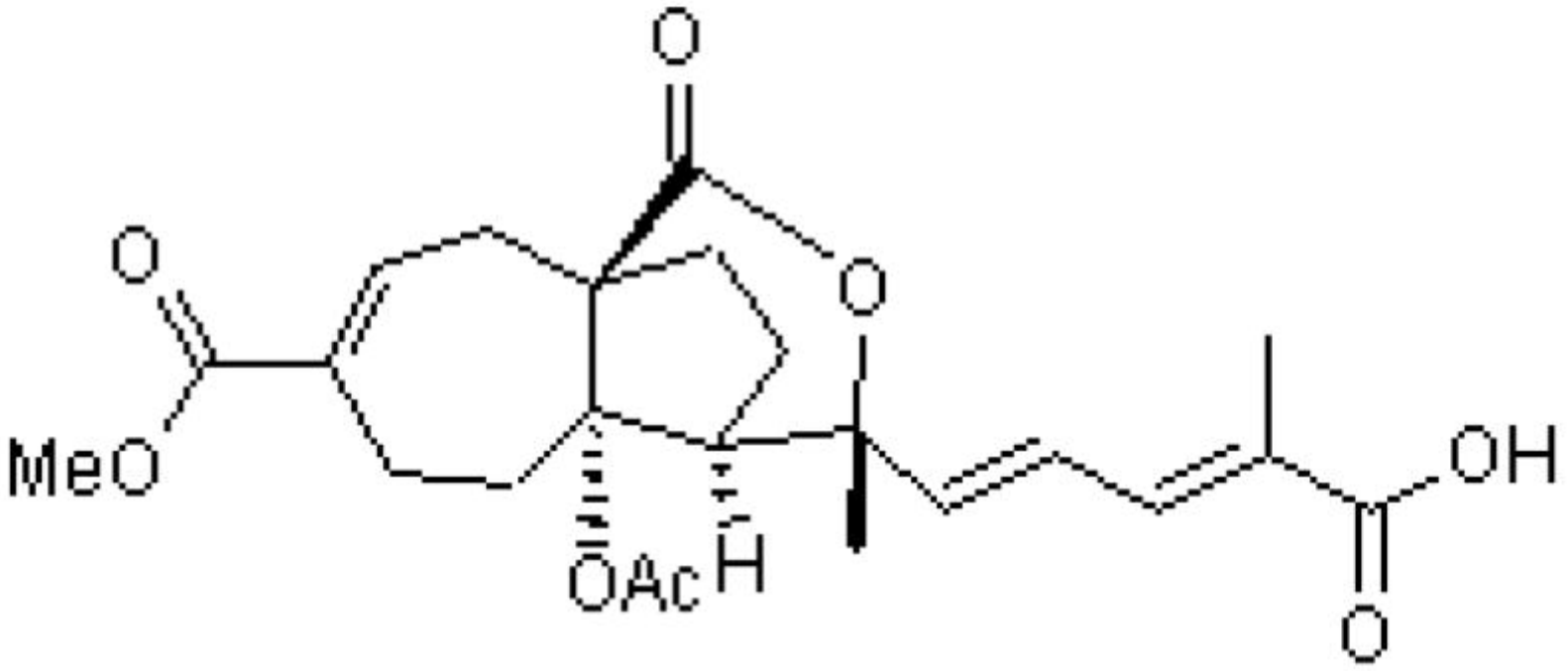

Figure 2

(a)

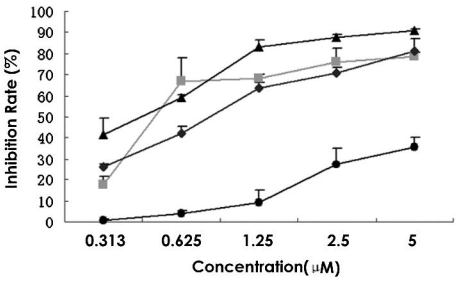

(b)

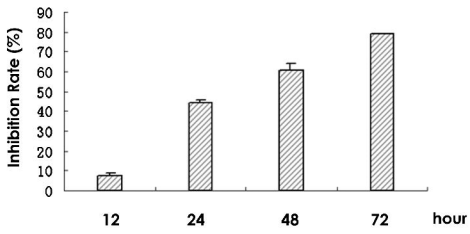

(c)

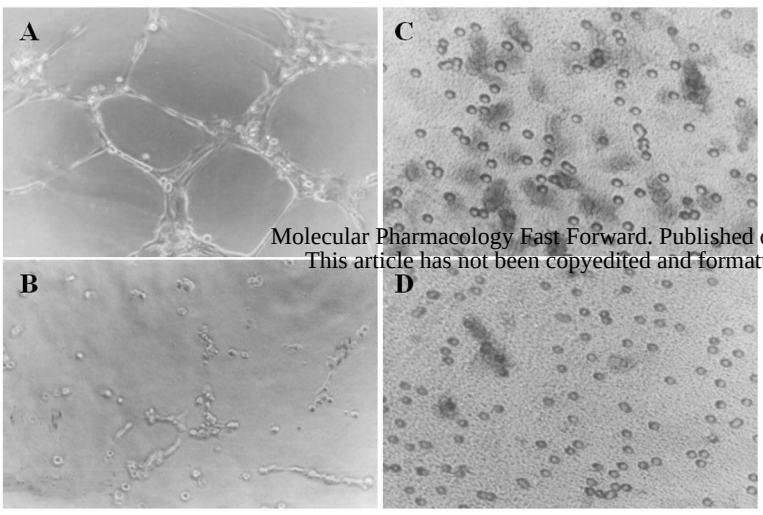

(d)

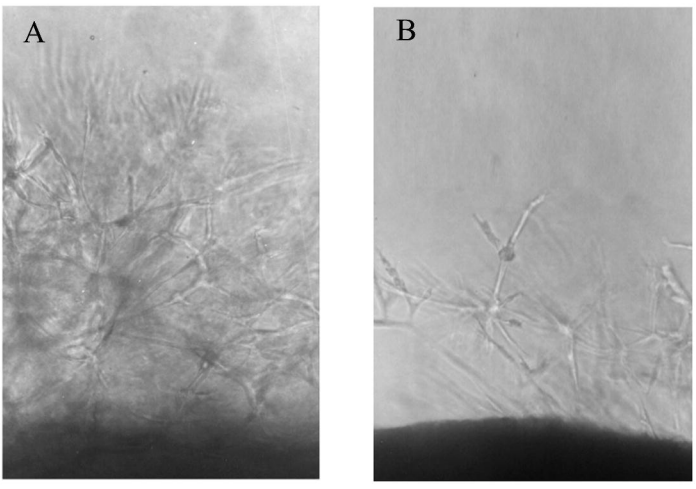

(e)

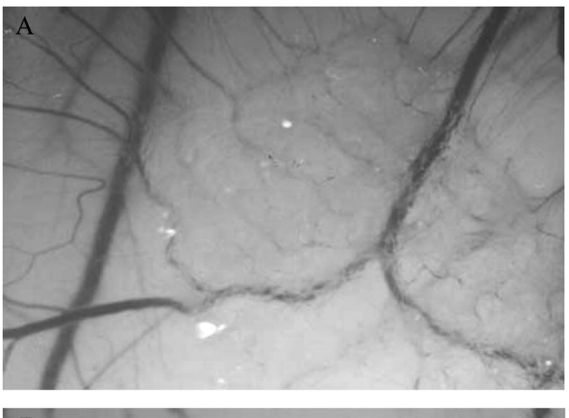

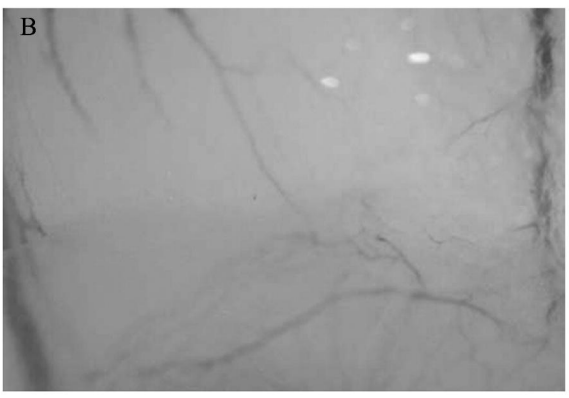

C

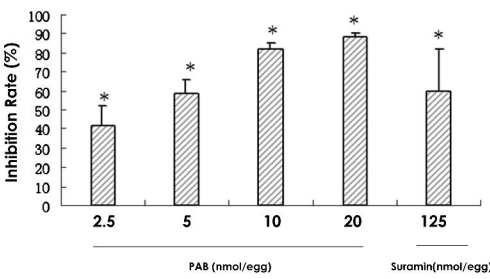

Figure 3

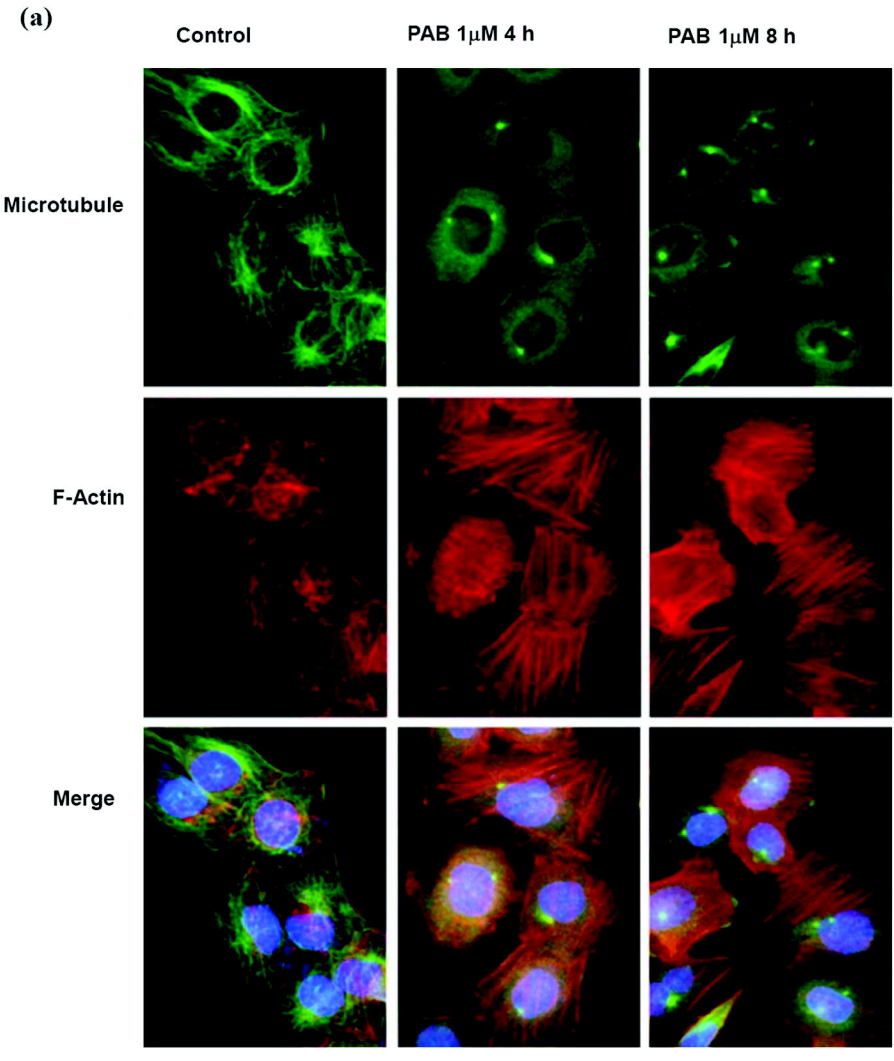
(a)
Control
PAB 1μM 4 h
PAB 1μM 8 h
Microtubule
F-Actin
Merge
(b)
Control
PAB
Cell Morphology
(c)
Increasement of F-/G-actin ratio
0
0. 5
1
1. 5
2
2. 5
3
3. 5
4
0
10min
30min
1h
4h
8h
16h
Time

Figure 4

(a)

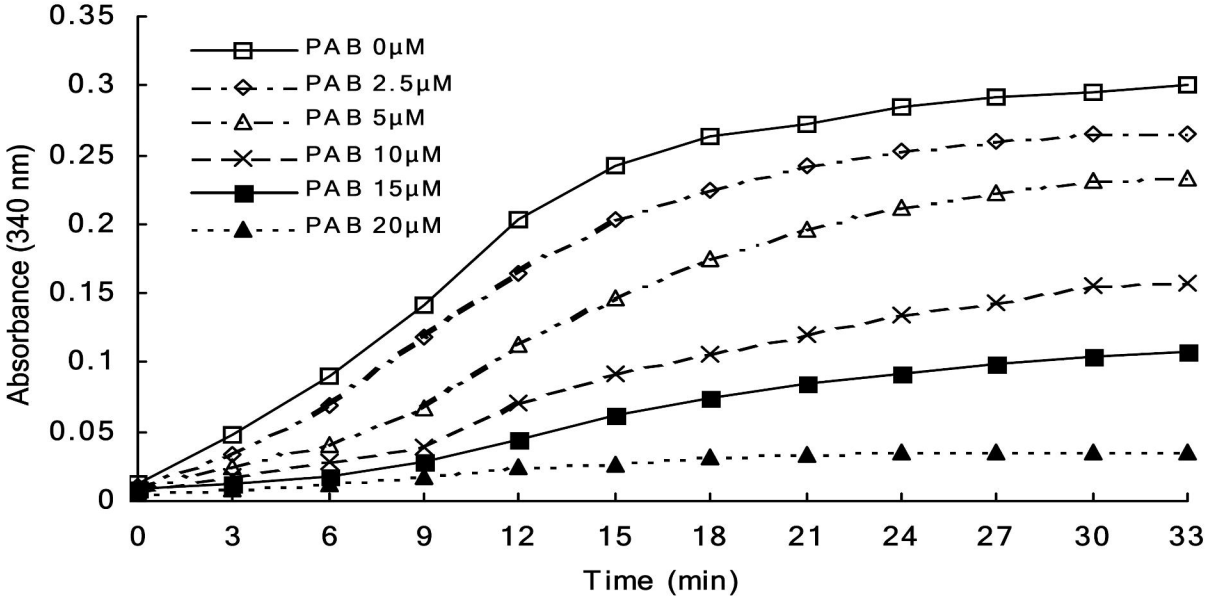
PAB 0μM
PAB 2.5μM
PAB 5μM
PAB 10μM
PAB 15μM
PAB 20μM
Absorbance (340 nm)
Time (min)
0.35
0.3
0.25
0.2
0.15
0.1
0.05
0
0
3
6
9
12
15
18
21
24
27
30
33

(b)

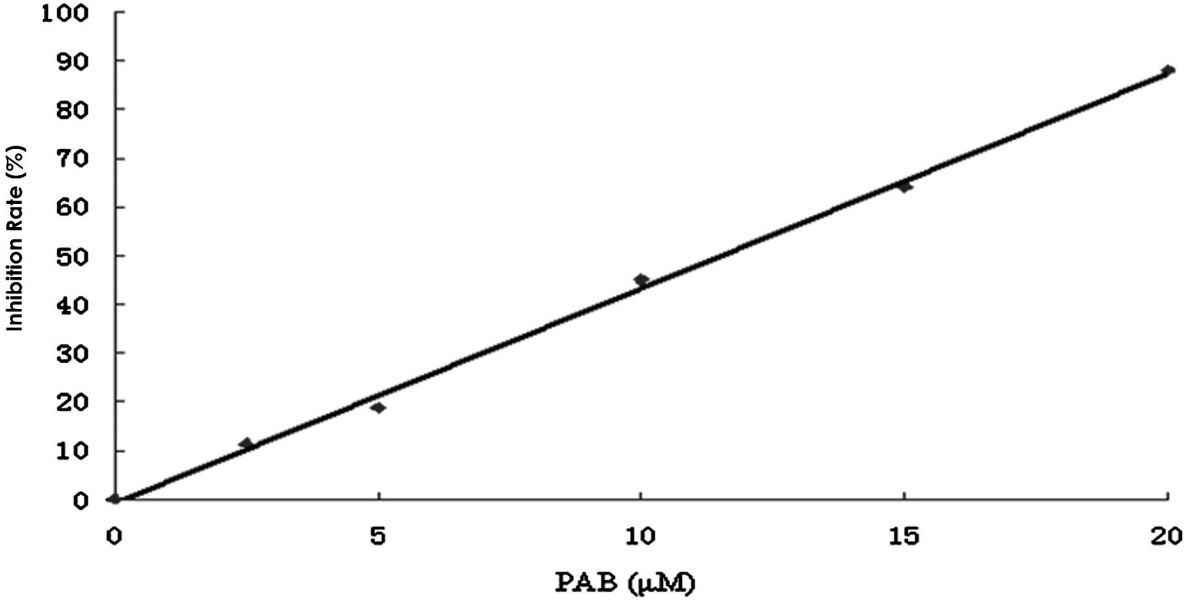
Inhibition Rate (%)
PAB (μM)
100
90
80
70
60
50
40
30
20
10
0
0
5
10
15
20

Figure 5

(a)

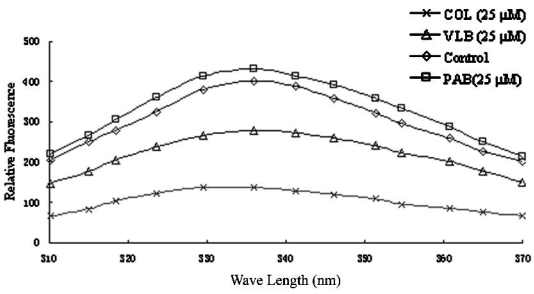

(b)

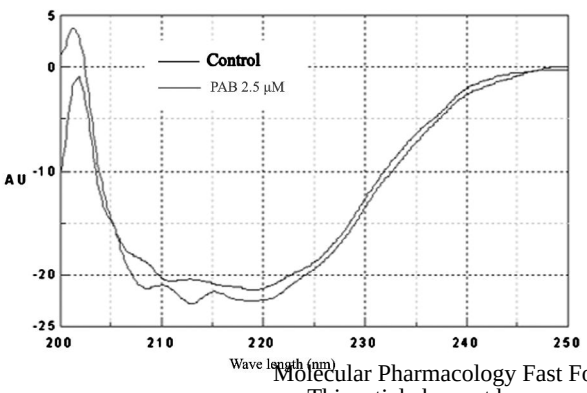

(c)

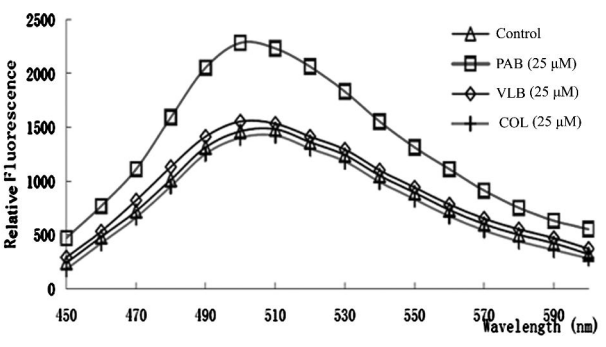

(d)

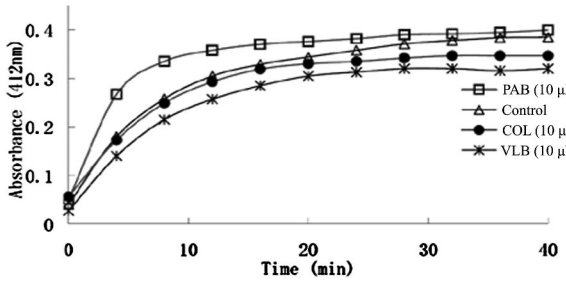

(e)

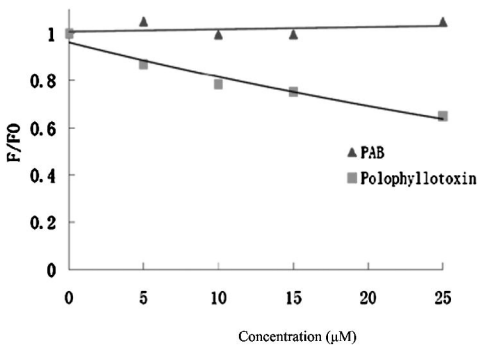

(f)

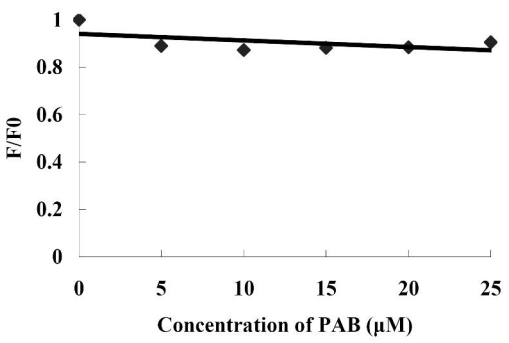

(g)